Supporting Information

Electrochemical hydrogenated TiO_2 nanotube arrays decorated with 3D Cotton-like porous MnO_2 enables superior supercapacitive performance

Jiaqin Liu[1,3,4*], Juan Xu[1,2], Yan Wang[1,3], Jiewu Cui[1,3], Hark Hoe Tan[4], Yucheng Wu[1,3*]

1 School of Materials Science and Engineering, Hefei University of Technology, Hefei 230009, China
2 School of Chemistry and Chemical Engineering, Hefei University of Technology, Hefei 230009, China
3 Key Laboratory of Advanced Functional Materials and Devices of Anhui Province, Hefei 230009, China
4 Department of Electronic Materials Engineering, Research School of Physics and Engineering, The Australian National University, Canberra, ACT 2601, Australia

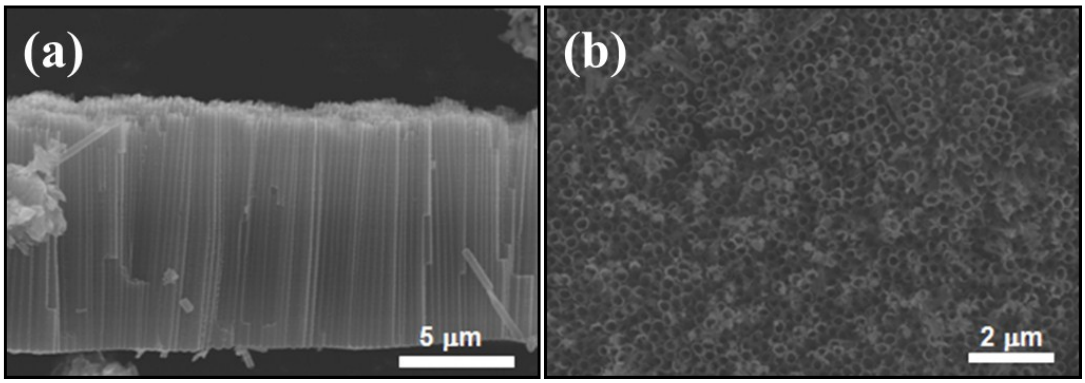

Fig. S1 (a) Side-view FESEM images of TNTAs and (b) overall view FESEM image of MnO_2/EH-TNTAs

Table. S1 Fitting results of three different TNTAs electrodes based on the equivalent circuit

Samples	R_s/ohm	R_{ct}/ohm	CPE/(F·cm^{-2})	Z_w/ohm
air-TNTAs	9.88	1475.0	0.00119	0.00499
H_2-TNTAs	7.42	279.20	0.02353	0.04770
EH-TNTAs	6.41	22.38	0.14770	0.01376

Capacitances calculated from CV curves:

The capacitances of electrodes were calculated from the CV curves according to the following equations:

$$C_s = \frac{S}{2 \times U \times \Delta V \times S_w}, C_m = \frac{S}{2 \times U \times \Delta V \times m}$$

where C_s (mF·cm^{-2}) refers to the areal capacitances of air-TNTAs, H_2-TNTAs and EH-TNTAs electrodes, S (A×V) is the integral area of CV curves, U (V·s^{-1}) is the scan rates, ΔV (V) is the potential window, S_w (cm^2) is the surface area of the air-TNTAs, H_2-TNTAs and EH-TNTAs electrodes; C_m (F·g^{-1}) refers to the specific capacitances of MnO_2/air-TNTAs, MnO_2/H_2-TNTAs and MnO_2/EH-TNTAs electrodes, and m is the mass of MnO_2.

Capacitances calculated from CD curves:

The capacitances of electrodes measured by galvanostatic charge/discharge method were calculated based on the following equations:

$$C_S = \frac{I \times \Delta t}{\Delta V \times S_w}, C_m = \frac{I \times \Delta t}{\Delta V \times m}$$

Where C_S (mF·cm^{-2}) refers to the areal capacitance of air-TNTAs, H_2-TNTAs and EH-TNTAs electrodes, I (A) is the constant discharging current, Δt is the discharging time, ΔV (V) is the potential window, and S_w (cm^2) is the surface area of the air-TNTAs, H_2-TNTAs and EH-TNTAs electrodes; C_m (F·g^{-1}) refers to the specific capacitance of MnO_2/air-TNTAs, MnO_2/H_2-TNTAs and MnO_2/EH-TNTAs electrodes, and m is the mass of MnO_2.

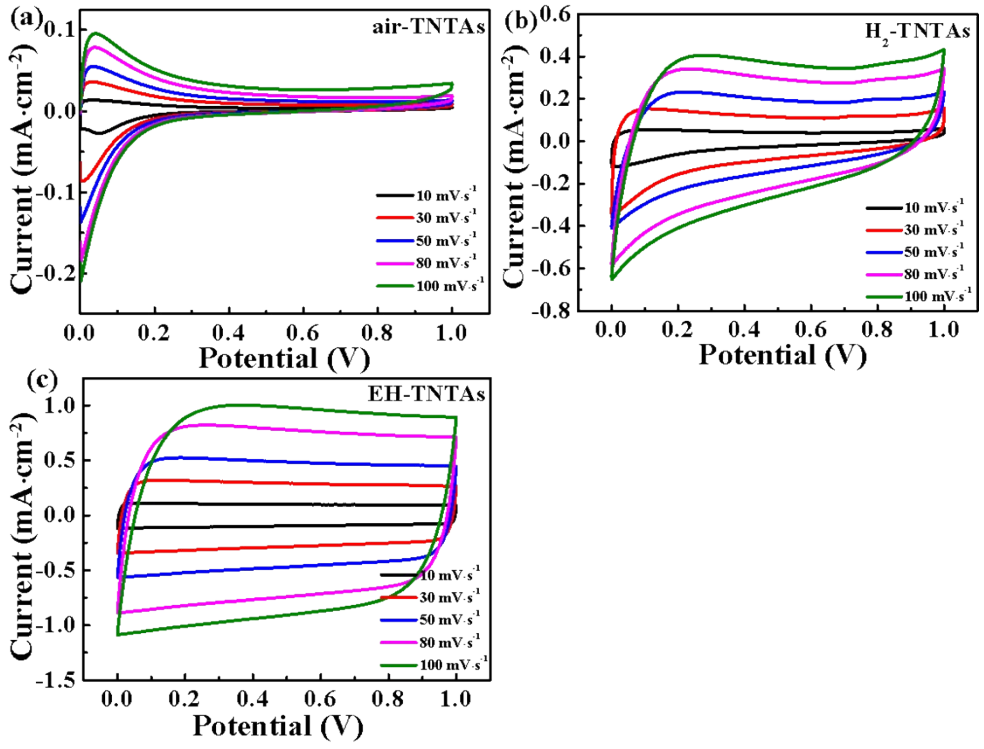

Fig. S2 CV curves of the (a) air-TNTAs, (b) H_2-TNTAs and (c) EH-TNTAs electrodes at different scan rates

Table. S2 Areal capacitance of air-TNTAs, H_2-TNTAs and EH-TNTAs at different scan rates

scan rates ($mV \cdot s^{-1}$)	Air-TNTAs ($mF \cdot cm^{-2}$)	H_2-TNTAs ($mF \cdot cm^{-2}$)	EH-TNTAs ($mF \cdot cm^{-2}$)
10	0.37	4.11	7.76
30	0.29	3.81	7.55
50	0.25	3.50	7.38
80	0.20	3.27	7.15
100	0.18	3.14	6.96

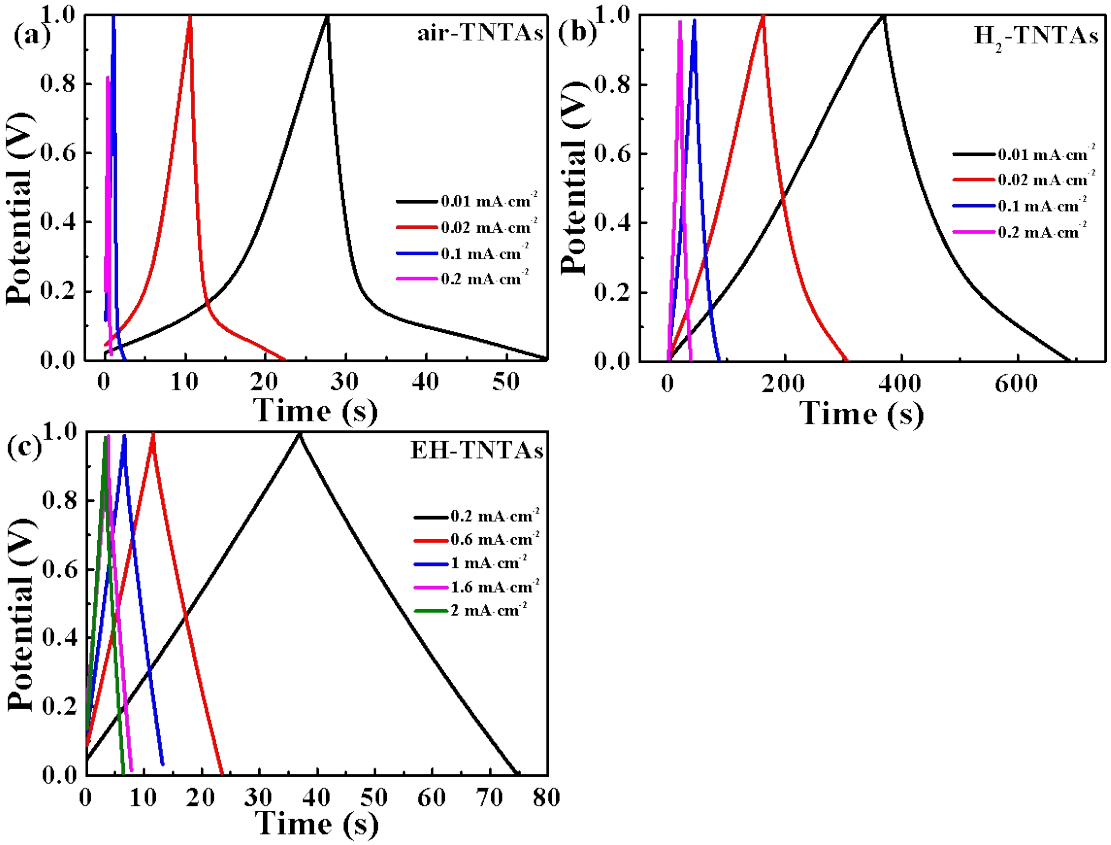

Fig. S3 GCD curves of the (a) air-TNTAs, (b) H_2-TNTAs and (c) EH-TNTAs electrodes at different current densities

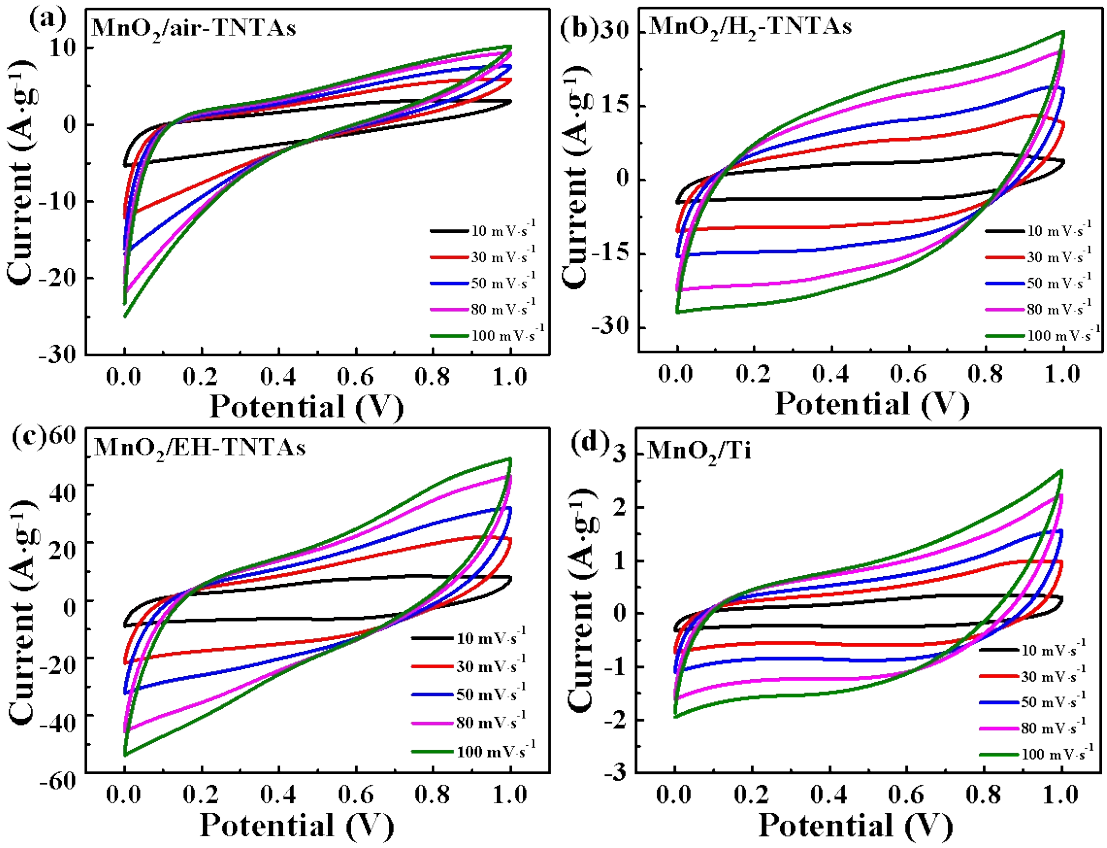

Fig. S4 CV curves of (a) MnO_2/air-TNTAs, (b) MnO_2/H_2-TNTAs, (c) MnO_2/EH-TNTAs and (d) MnO_2/Ti electrodes at different scan rates

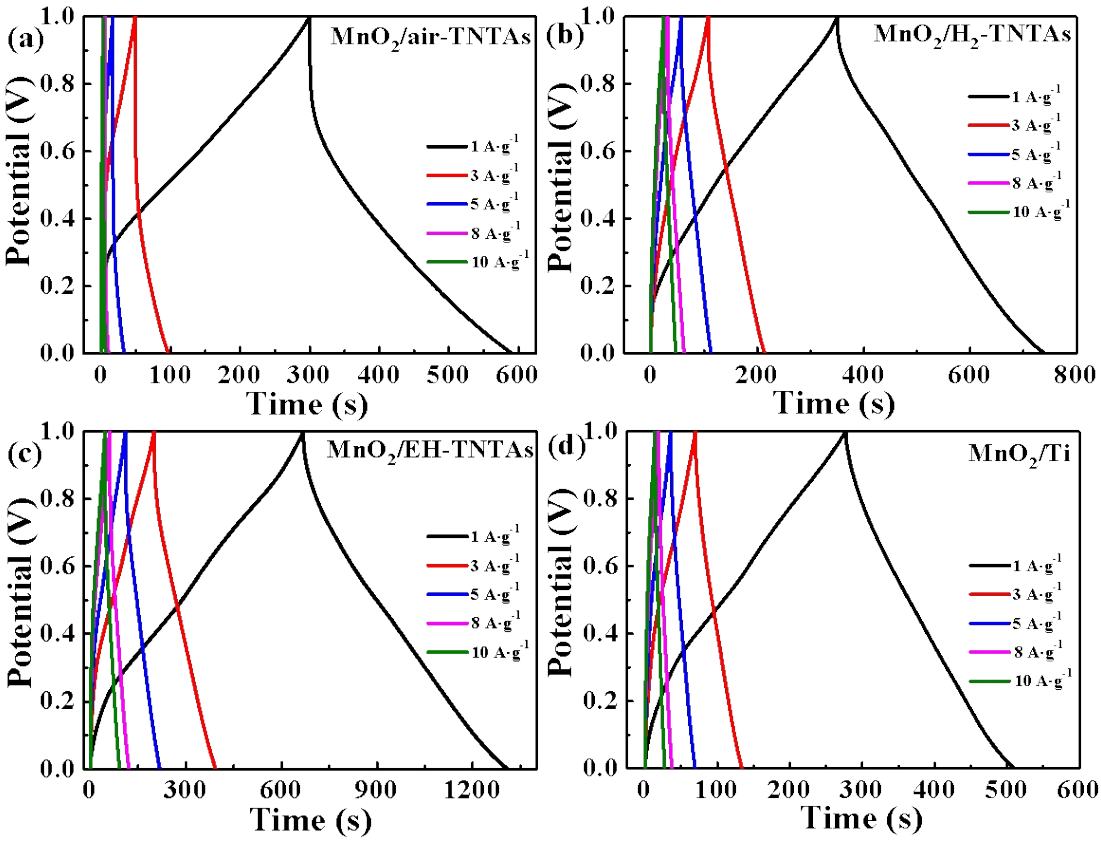

Fig. S5 GCD curves of (a) MnO_2/air-TNTAs, (b) MnO_2/H_2-TNTAs, (c) MnO_2/EH-TNTAs and (d) MnO_2/Ti electrodes at different current densities

Table. S3 Mass of pseudo-capacitive material and the specific capacitance for MnO_2-based electrode with different substrates

Sample	Mass of MnO_2 /(mg·cm^{-2})	Specific capacitance /(F·g^{-1}) at 1 A·g^{-1}	Specific capacitance /(F·g^{-1}) at 10 mV·s^{-1}
MnO_2/Ti foil	0.20	257.7 F·g^{-1}	205.8 F·g^{-1}
MnO_2/air-TNTAs	0.16	290.7 F·g^{-1}	218.8 F·g^{-1}
MnO_2/H_2-TNTAs	0.10	388.7 F·g^{-1}	326.4 F·g^{-1}
MnO_2/EH-TNTAs	0.12	650.0 F·g^{-1}	558.9 F·g^{-1}
EH-TNTAs@MnO_2	0.20	523.9 F·g^{-1}	469.1 F·g^{-1}

Table. S4 Performance comparison of reported electrode materials composed of various supports and MnO_2 deposit

Electrode materials	Technique	Electrolyte	Capacitance (F/g)	Stability (cycles)	Ref.
MnO_2/C@TiO_2 NTAs	C larger coating and hydrothermal deposition of MnO_2	1.0 M Na_2SO_4	521.4 (2 A/g)	88.6% (2000)	2016[1]
MnO_2@TNTAs	Pulsed electrodeposition of MnO_2	0.5 M Na_2SO_4	425.0 (0.5 A/g)	71.4% (3000)	2016[2]
MnO_2/H_2-TiO_2/ C microfiber	Hydrogen annealing and hydrothermal deposition of MnO_2	0.5 M Na_2SO_4	630.1 (10 mV/s)	90.0% (5000)	2015[3]
H_2-TiO_2 NTAs/C/MnO_2	Hydrogen treatment, carbon coating and hydrothermal deposition of MnO_2	1.0 M Na_2SO_4	299.8 (0.5 A/g)	87.0% (2000)	2015[4]
MnO_2-TiO_2/C NTAs	C coating and potentiostatic deposition of MnO_2	0.5 M Na_2SO_4	580.0 (2.6 A/g)	90.0% (1000)	2014[5]
MnO_2/C/TiO_2 nanowire arrays	C coating and electrodepositing MnO_2	0.5 M Na_2SO_4	639.0 (1 A/g)	78.7% (1000)	2014[6]
MnO_2@TiO_2 nanobelt arrays	Hydrothermal deposition of MnO_2	1.0 M Na_2SO_4	557.6 (200 mV/s)	86.3% (3000)	2013[7]
H_2-TiO_2@MnO_2 nanowires	Hydrogen annealing and anodic electrodeposition of MnO_2	5.0 M LiCl	449.6 (10 mV/s)	91.2% (5000)	2013[8]

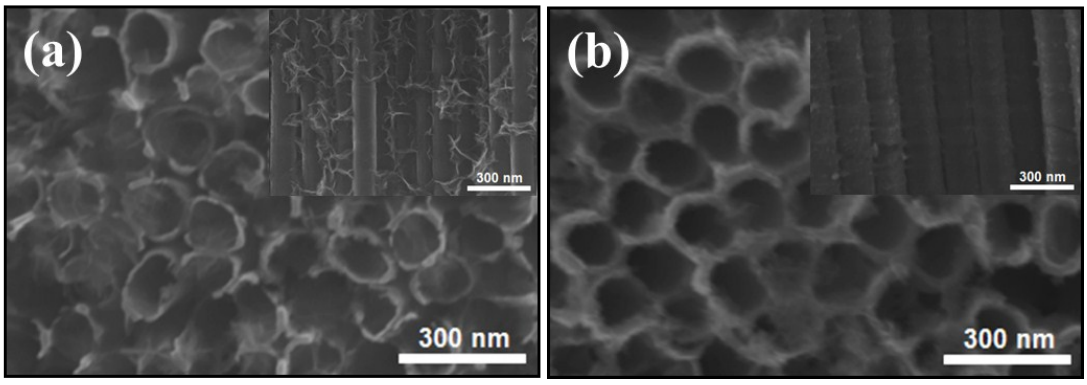

Fig. S6 FESEM images of (a) MnO_2/EH-TNTAs and (b) EH-TNTAs@MnO_2 (insets are the corresponding side-view images)

Table. S5 The relative BET specific surface area of EH-TNTAs, MnO_2/EH-TNTAs and EH-TNTAs@MnO_2

sample	Relative BET specific surface area (m^2/cm^2)
EH-TNTAs	0.2124
MnO_2/EH-TNTAs	0.3326
EH-TNTAs@MnO_2	0.2677

Note: Regarding to the measuring and calculation methods for the relative BET specific surface area please refer to reference [9].

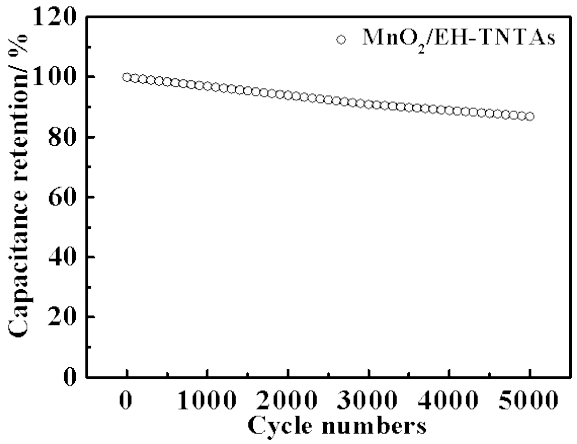

Fig. S7 Cycling performance of the MnO_2/EH-TNTAs electrode at a current density of 5 $A \cdot g^{-1}$

References

1. Z. Wang, Y. Wang, X. Shu, C. Yu, J. Zhang, J. Cui, Y. Qin, H. Zheng, Y. Zhang and Y. Wu, *RSC Adv.*, 2016, **6**, 63642-63651.
2. H. Zhou, X. Zou and Y. Zhang, *Electrochimica Acta*, 2016, **192**, 259-267.
3. X. Y. Cao., X. Xing., N. Zhang., H. Gao., M. Y. Zhang., Y. C. Shang. and X. T. Zhang, *Journal of Materials Chemistry And Physics*, 2015, **3**, 3785-3793.
4. J. Di, X. Fu, H. Zheng and Y. Jia, *Journal of Nanoparticle Research*, 2015, **17**, 1-12.
5. B. Gao, X. Li, Y. Ma, Y. Cao, Z. Hu, X. Zhang, J. Fu, K. Huo and P. K. Chu, *Thin Solid Films*, 2014, DOI: 10.1016/j.tsf.2014.09.071.
6. SainanYang, K. Cheng, J. Huang, K. Ye, Y. Xu, D. Cao and X. Z. G. Wang, *Electrochimica Acta*, 2014, **120**, 416-422.
7. Y. Luo, D. Kong, J. Luo, S. Chen, D. Zhang, K. Qiu, X. Qi, H. Zhang, C. M. Li and T. Yu, *RSC Advances*, 2013, **3**, 14413–14422.
8. X. Lu, M. Yu, G. Wang, T. Zhai, S. Xie, Y. Ling, Y. Tong and Y. Li, *Adv Mater*, 2013, **25**, 267-272.
9. J. Liu, L. Ruan, S.B. Adeloju and Y. Wu, Dalton Trans., 2014, **43**, 1706-1715.